International Journal of Science and Research (IJSR)
ISSN: 2319-7064
Impact Factor 2025: 7.089

Petrophysical and Gas-Logging Evaluation of Reservoir Quality and Hydrocarbon Distribution in the Sokor-1 Formation, Agadi Prospect, Termit Basin, Southeastern Niger

M.A.I. Ari[1], M.E. Nton[2], M. Harouna[3]

[1]Petroleum Geosciences Program, Pan African University Life and Earth Sciences Institute (including Health and Agriculture), Ibadan, Oyo State, Nigeria

[2]Department of Geology, University of Ibadan, Ibadan, Oyo State, Nigeria

[3]Department of Geology, Abdou Moumouni University, Niamey, Niger

Abstract: ***The Sokor-1 Formation is an important reservoir succession within the petroleum system of the Termit Basin, southeastern Niger. This study integrates wireline logs and gas data from two wells in the Agadi Prospect to evaluate reservoir quality and hydrocarbon distribution. Shale volume, porosity, permeability, water saturation, hydrocarbon saturation, gas concentration, porosity-permeability relationships, and reservoir quality were assessed. The investigated intervals exhibit substantial vertical and lateral heterogeneity. Reservoir units in well A-7 generally display higher porosity and permeability and stronger gas indications than those in well B-14. Hydrocarbon saturation is locally high, whereas the deeper intervals in well B-14 generally exhibit poorer flow properties. Porosity and permeability show a positive relationship, although the observed scatter indicates additional controls related to shale content, facies variability, pore connectivity, and diagenesis. Reservoir units A1, A2, A10, A13, and A14 are among the most favorable intervals, whereas B6-B8 show comparatively poor reservoir quality. The integrated evaluation demonstrates that the most prospective intervals occur where favorable porosity and permeability coincide with relatively low shale and water saturation and high hydrocarbon saturation. These results support reservoir zonation and the identification of prospective intervals in the Agadi Prospect. Additional wells, complemented by core, pressure, fluid, and production data, are recommended to reduce subsurface uncertainty and better constrain the spatial distribution of reservoir quality and hydrocarbon accumulation across the Agadi Prospect.***

Keywords: Wireline logs; Gas logging; Reservoir quality; Hydrocarbon distribution; Sokor-1 Formation; Agadi Prospect, Termit Basin

1. Introduction

The West and Central African Rift System (WCARS) is a major intracontinental Meso-Cenozoic rift system comprising several extensional and strike-slip basins (Fig. 1). Its development was mainly related to the fragmentation of Gondwana and the differential movement of African crustal blocks associated with the opening of the South and Central Atlantic and Indian Oceans (Genik, 1993; Zanguina et al., 1998). The Termit Basin forms part of the western WCARS (Fig. 1) and hosts a proven petroleum system, particularly within the Agadem Block, where commercial oil production began in 2011. The basin contains several source, reservoir, and seal units. The main source rocks include the Upper Cretaceous Donga and Yogou formations and Paleogene lacustrine mudstones of the Sokor-1 and Sokor-2 formations. Hydrocarbons occur mainly in the Sokor-1, Yogou, and Madama formations, with Sokor-1 representing an important multilayered reservoir succession composed of interbedded sandstones and mudstones. The overlying Sokor-2 lacustrine shales provide an important regional seal (Genik, 1993; Zanguina et al., 1998; Harouna & Philp, 2012 ; Wan et al., 2014).

ISSN: 2319-7064
Impact Factor 2025: 7.089

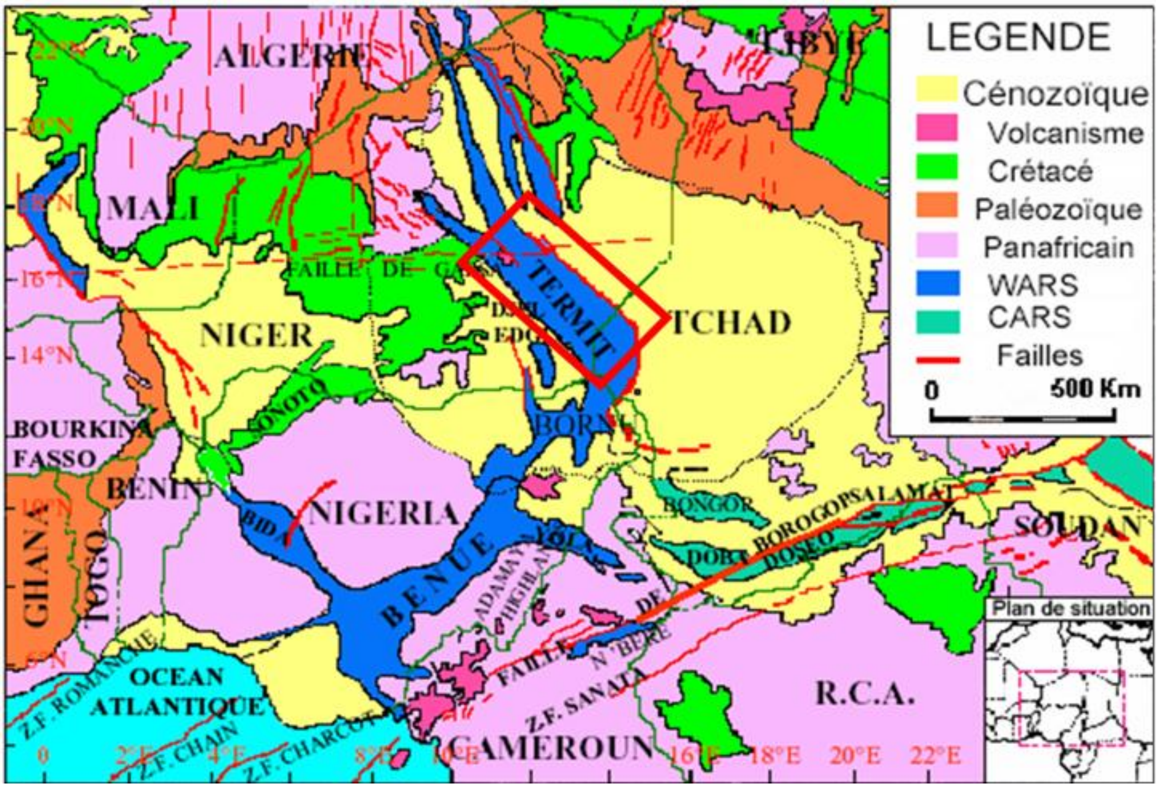

Figure 1: Regional geographic map of the West and Central African Rift System with the location of the Termit Basin (Genik 1993).

The heterogeneous nature of Sokor-1 requires detailed evaluation of its petrophysical properties to distinguish effective reservoir intervals. Well logs provide continuous measurements that allow shale volume, porosity, permeability, and fluid saturation to be estimated from the integrated interpretation of gamma-ray, resistivity, density, and neutron logs (Krygowski, 2004; Schlumberger, 1989). Gas data provide additional evidence for hydrocarbon-bearing intervals and can therefore complement the petrophysical assessment. Despite extensive exploration and geological studies of the reservoirs in the Termit Basin (Hamma & Harouna, 2019; Amadou et al., 2021a, 2021b; Chang & Zung, 2017; Nasaruddin et al., 2017; Hamma et al., 2022; Ari et al., 2024, 2026), the petrophysical variability and quality of individual Sokor-1 reservoir intervals remain insufficiently constrained, particularly in the Agadi Prospect. This study integrates well-log and gas data from Wells A-7 and B-14 to evaluate the petrophysical characteristics and reservoir quality of the Sokor-1 Formation. It focuses on shale volume, porosity, permeability, water and hydrocarbon saturation, gas distribution, and their relationships to identify the most favorable reservoir intervals in the Agadi Prospect (Fig. 2), Termit Basin, southeastern Niger (Fig. 1).

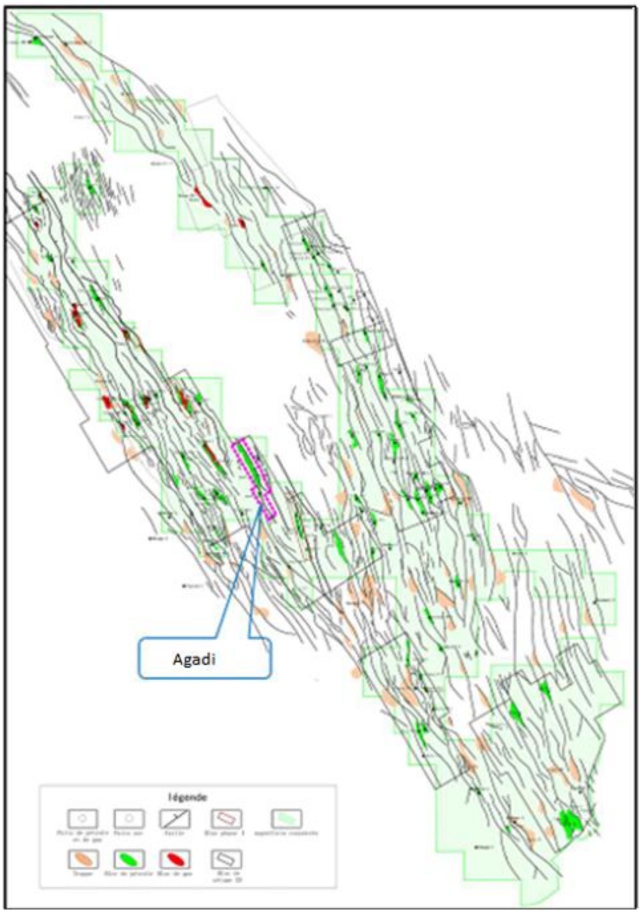

Figure 2: Location map of Agadi prospect

2. Geological Context of the Termit Basin

The Termit Basin is a Mesozoic-Cenozoic intracontinental rift basin within the western sector of the West and Central African Rift System (Fig. 1). Its evolution records successive phases of rifting, thermal subsidence, tectonic reactivation, and uplift from the Pan-African orogeny (750-550 Ma) to the Neogene. The sedimentary succession overlies Precambrian to Jurassic crystalline and metamorphic basement (Fig. 3). The Lower Cretaceous to Quaternary sedimentary succession locally reaches approximately 14,000 m (Genik, 1993). The main rifting phase occurred during the Early to Late Albian and was followed by rapid thermal subsidence, thereby generating extensive accommodation space for fluvial-to-lacustrine sedimentation (Bosworth, 1992; Genik, 1993; Schull, 1988; Zanguina et al., 1998). The Upper Cretaceous succession includes the Donga, Yogou, and Madama formations (Fig. 3). During the Cenomanian-Campanian, marine incursions through connections with the Neo-Tethys to the north and the South Atlantic through the Benue Trough to the south produced alternating marine-influenced and continental depositional conditions (Philip, 1993; Wilson & Guiraud, 1992). Progressive restriction of these connections during the Campanian favored the accumulation of organic-rich shales, particularly within the Yogou Formation (Fig. 3), which represents an important source-rock interval (Zhao et al., 2019).

The Paleogene was characterized by renewed tectonic activity and fault reactivation, resulting in differential subsidence and variations in accommodation space (Wang et al., 2017; Wilson & Guiraud, 1992). Within this tectonically active setting (Fig. 4), the Sokor-1 and Sokor-2 formations accumulated as deltaic to lacustrine successions dominated by interbedded sandstones and mudstones (Fig. 3). Their distribution and thickness were strongly controlled by syn-sedimentary faulting, which influenced depocentre development, sediment-transport pathways, and the distribution of sandy and muddy facies within the Sokor-1 Formation.

The present structural framework is dominated by extensional and transtensional fault systems (Genik, 1993; Zanguina et al., 1998), particularly NW-SE- and NNW-SSE-trending structures (Fig. 2). These include Early Cretaceous faults reactivated during the Paleogene and faults developed (Fig. 4) during the Paleogene, affecting both Upper Cretaceous and Paleogene strata (Ji-Lin et al., 2012).

3. Dataset and Methods

3.1 Dataset

The data used in this study are the gas data and wireline logs from the Sokor-1 Formation. These data from wells A-7 and B-14 include gamma-ray (GR), resistivity (LLD), neutron, and density logs.

Paper ID: SR26823144710 DOI: https://dx.doi.org/10.21275/SR26823144710

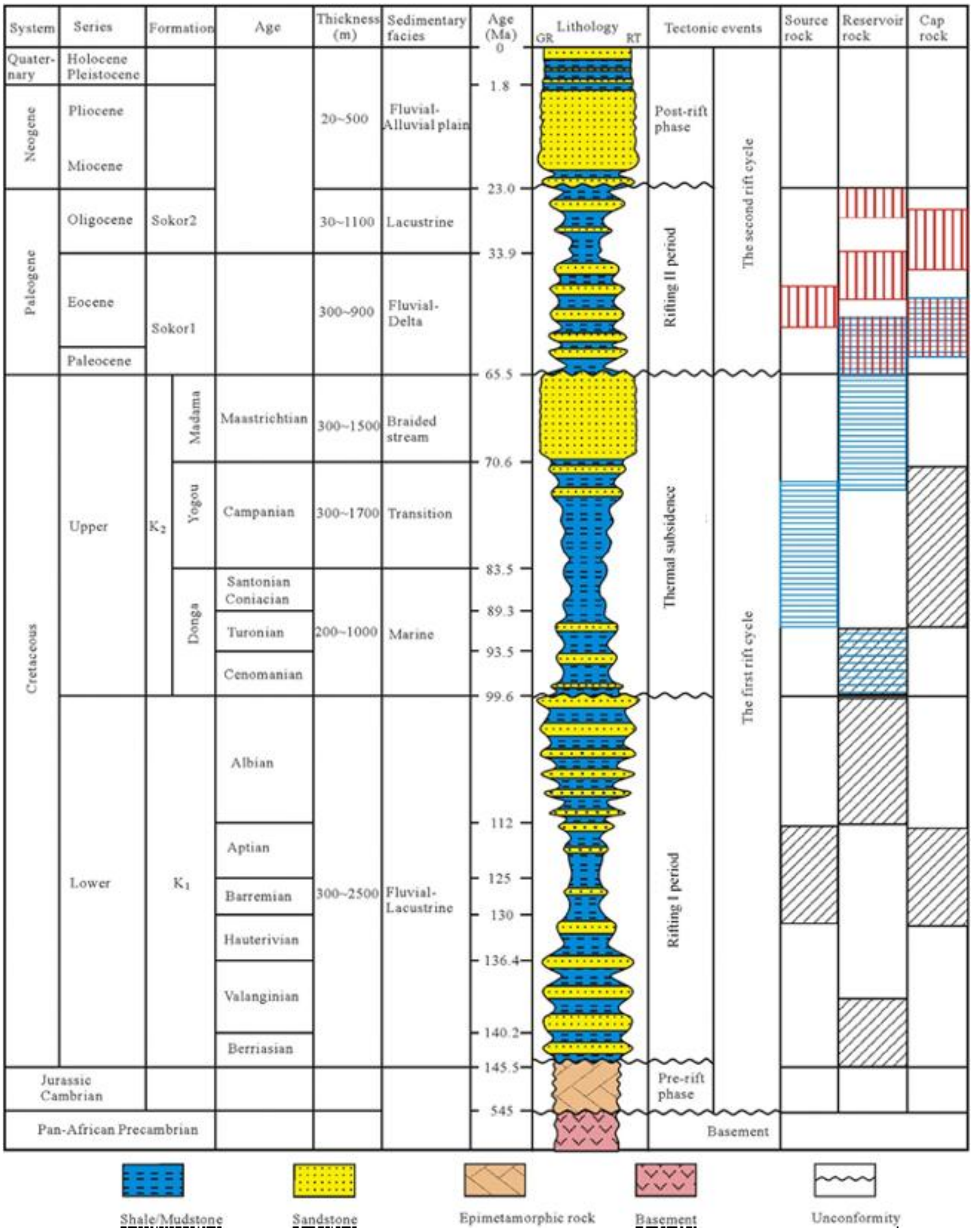

Figure 3: Stratigraphic column, tectonic events and petroleum system of the Termit Basin, Niger (After Wan et al., 2014).

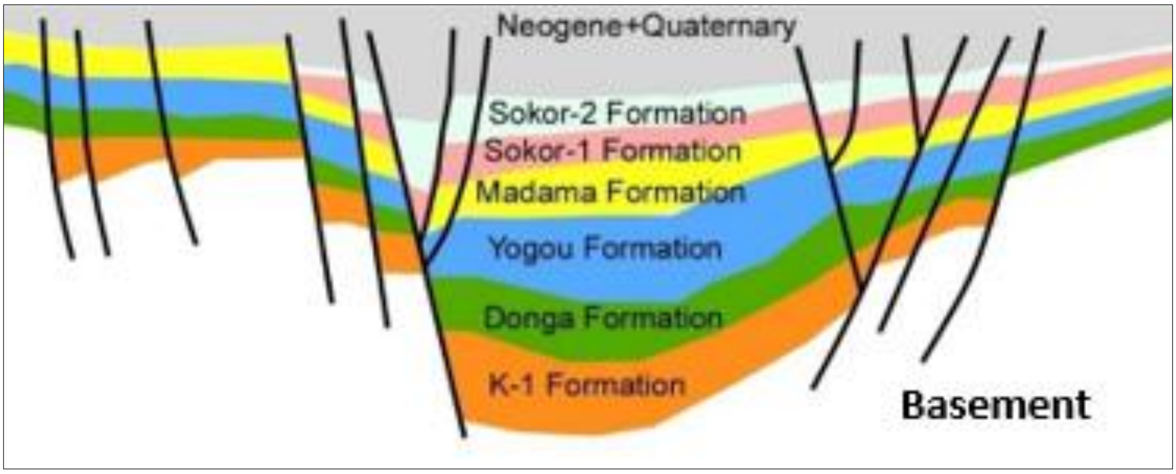

Figure 4: Structural cross-section in the Termit Basin showing the rift architecture

3.2 Methods

Reservoir units from the Sokor-1 Formation were identified by using the gamma-ray logs combined with resistivity, neutron, and density logs (Krygowski, 2004; Cannon, 2016; Darling, 2005). Standard petrophysical interpretation techniques were used to evaluate the reservoir petrophysical properties of the wells. In this work, the parameters determined are volume of shale (Vsh), porosity (Φ), permeability (k), water saturation (Sw), and hydrocarbon saturation (Sh).

The shale volume (Vsh) was calculated using the Larionov formula (1969), as the Sokor-1 Formation is a Tertiary sedimentary rock.

$$IGR = \frac{Grlog - Grmin}{Grmax - Grmin} \quad (1)$$

$$Vsh = 0.083 * (2^{3.7*IGR} - 1) \quad (2)$$

Where:
IGR = Gamma-ray index; GRlog = Gamma-ray log reading in the zone of interest; GRmax = Maximum gamma-ray reading for the shale; GRmin = Minimum gamma-ray reading for the clean sand.

Porosity was calculated from the bulk-density log using the standard density-porosity relationship:

$$\text{Porosity } (\Phi) = \frac{\rho ma - \rho b}{\rho ma - \rho f} \quad (3)$$

Where: Φ is the total porosity (%), ρma is the matrix density (g/cm³), bulk density is the formation bulk density obtained from the density log (g/cm³), and ρf is the pore-fluid density (g/cm³). A matrix density of 2.65 g/cm³ was adopted for the reservoir intervals, whereas the fluid density was estimated from the neutron-density crossplot.

The shale porosity was estimated using:

$$\Phi sh = \frac{\rho ma - \rho sh}{\rho ma - \rho f} \quad (4)$$

where Φsh is the apparent porosity of the shale (%), and ρsh is the bulk density of the shale (g/cm³)

Effective porosity was then calculated by correcting the total porosity for the contribution of shale:

$$\Phi E = \Phi - (\Phi sh * VSh) \quad (5)$$

where ΦE is the effective porosity (%), Φ is the total porosity (%), Φsh is the shale porosity (%), and VSh is the shale volume (%). Shale volume was determined from the gamma-ray log using the method described previously.

Permeability was estimated empirically from porosity and irreducible water saturation using the Tixier (1949) relationship:

$$K = [\frac{(250 * \Phi 3}{Swir}]^2 \quad (6)$$

Where:
K is permeability (mD), Φ is porosity (%), and Swir is irreducible water saturation (%). The relationship was applied as an empirical log-derived permeability estimate and should therefore be regarded as an indirect estimate rather than a substitute for core-measured permeability.

The irreducible water saturation was calculated using the Schlumberger empirical relationship:

$$Swir = (F/200)^{1/2} \quad (7)$$

Where: Swir is irreducible water saturation (%) and F is the formation factor (dimensionless). The formation factor was calculated from porosity according to:

$$F = \frac{a}{\Phi\text{^}2} \quad (8)$$

Where: a is the tortuosity factor (dimensionless), Φ is porosity (%), and m is the cementation exponent (dimensionless).

Water saturation was calculated using the Archie (1942) equation:

$$Sw = \sqrt[n]{\frac{Rw.F}{Rt}} \quad (9)$$

Where:
Sw=the water saturation (%); a=the tortuosity factor (dimensionless); Rw represents the degree of water resistivity (Ohm.m); Rt=the true resistivity of the hole (Ohm.m); F = the formation factor (dimensionless); m is the cementation exponent (dimensionless), and n is the saturation exponent (dimensionless). The Archie parameters adopted in this study were (a=1), (m=2), and (n=2)

Hydrocarbon saturation (%) is calculated from water saturation (%) by the following equation.

$$\text{Hydrocarbon saturation (Sh)} = 1 - Sw \quad (10)$$

The Reservoir Quality Index (RQI) was calculated using the conventional Amaefule et al. (1993) relationship:

$$RQI = 0.0314 \sqrt{\frac{K}{\Phi}} \quad (11)$$

With RQI is the reservoir quality index in µm; (K) is permeability (mD), and Φ is effective porosity expressed in %. The factor 0.0314 converts the expression to µm when permeability is expressed in mD and porosity in %. Thus, the RQI reported in this study represents the conventional Reservoir Quality Index, calculated from permeability and effective porosity, rather than a separately constructed integrated reservoir-quality index.

4. Results

4.1 Petrophysical characteristics of the reservoir intervals

The petrophysical evaluation of the Sokor-1 reservoir intervals reveals substantial variations in shale volume, porosity, permeability, and fluid saturation (Table 1) between the shallow reservoir units of well A-7 (1890-2095 m) and the deeper reservoir units of well B-14 (2098-2204 m) (Fig. 5A-E). The reservoir units of well A-7 generally exhibit better reservoir properties than those of well B-14.

The shale volume (Vsh) ranges from 10.0 to 33.0% in the reservoir units of well A-7, with an average of 17.57%, whereas the reservoirs of well B-14 range from 6.73 to 52.74%, averaging 21.90% (Table 1). Most reservoirs of well A-7 therefore contain relatively low to moderate shale contents, although reservoir unit A6 reaches 33% (Table 1). In the reservoir B intervals, reservoir unit B8 exhibits the highest shale volume (52.74%), indicating a substantially more argillaceous reservoir zone (Table 1). The Vsh profiles (Fig. 5A) show that the deepest reservoir units of well B-14 are generally associated with higher shale content and poorer reservoir development.

Porosity varies from 16.88 to 38.73% in the reservoir units of well A-7, with an average of 24.37% (Table 1), compared with 7.76-26.80% and an average of 17.51% in the reservoir units of well B-14 (Fig. 5B). The porosity values range from 17% to 30% (Nasaruddin et al., 2017), whereas Genik (1993) found 25-35%, and Amadou et al. (2021a) found high porosity (averaging 22.51% and up to 28.7%). The highest porosities occur in reservoir units A2 (38.73%) and A1 (36.38%), whereas reservoir unit B8 has the lowest value (7.76%). The progressive reduction in porosity toward the deeper reservoir units of well B-14 indicates deterioration of pore-space quality with depth.

Table 1: Petrophysical properties of reservoirs of the Sokor-1 Formation

Wells	Réservoir Units	Depth (m)		Vsh (%)	Φ (%)	K (mD)	SW (%)	Shc (%)
		From	To					
	A1	1890	1891	28	36.38	81.66	14.74	85.86
Well A-7	A2	1898	1900	19.64	38.73	146.26	9.93	90.07
	A3	1906	1908	28	24.44	16.84	21.67	78.33
	A4	1911	1913	12.87	22.39	7.65	36.64	63.36
	A5	1921	1923	16.1	18.1	4.71	31.45	68.55
	A6	1924	1926	33	16.88	4.93	24.38	75.62
	A7	1933	1937	12.87	25.31	4.62	87.79	12.21
	A8	1943	1945	18.18	29.44	16.37	38.96	61.04
	A9	1948	1950	19.64	25.44	5.61	73.38	26.62
	A10	1987	1991	19.64	26.94	85.9	5.69	94.31
	A11	1998	2000	12.87	19.86	6.83	28.66	71.34
	A12	2001	2003	12.87	18.65	6.14	26.43	73.57
	A13	2005	2008	12.87	20.15	9.41	21.74	78.26
	A14	2013	2015	11.7	23.86	27.14	12.51	87.49
	A15	2017	2021	10	21.65	4	63.5	36.5
	A16	2092	2095	12.87	21.65	7.62	33.28	66.72
	Average values			17,57	24,37	27,23	33,17	66,87
Well B-14	B1	2098	2100	19,64	20,13	13,63	14,96	85,04
	B2	2105	2109	22,22	20,39	11,84	16,5	83,5
	B3	2110	2112	12,9	26,8	43,74	11	89
	B4	2114	2116	25	10,81	1,13	28,04	71,96
	B5	2181	2183	6,73	14,57	3,41	22,67	77,33
	B6	2192	2194	19,64	20,13	12,94	15,76	84,24
	B7	2196	2197	16,37	19,49	11,35	16,31	83,69
	B8	2202	2204	52,74	7,76	0,27	43,89	56,11
	Average values			21,91	17,51	12,29	21,14	78,86

Permeability exhibits an even stronger heterogeneity (Fig. 5C). The reservoir units of well A-7 range from 4.00 to 146.26 mD, averaging 27.23 mD, while the reservoir units of well B-14 range from only 0.27 to 43.74 mD, with an average of 12.29 mD (Table 1). Reservoir unit A2 records the highest permeability (146.26 mD), followed by reservoir units A10 (85.90 mD) and A1 (81.66 mD). In contrast, reservoir unit B8 has an extremely low permeability of 0.27 mD, consistent with its low porosity and high shale volume.

The porosity-permeability crossplot (Fig. 5G) shows a clear positive relationship between porosity and permeability. For the complete dataset, the correlation coefficient is approximately $r = 0.77$, indicating that intervals with greater pore volume generally possess better fluid-flow capacity. However, the considerable scatter demonstrates that permeability is not controlled by porosity alone and is also influenced by shale content, pore connectivity, and diagenetic modification.

4.2 Water and hydrocarbon saturation

Water saturation (Sw) ranges from 5.69 to 87.79% in the reservoir units of well A-7 (Table 1) and from 11.00 to 43.89% in the reservoir units of well B-14 (Fig. 5D). The corresponding hydrocarbon saturation (Shc) ranges from 12.21 to 94.31% and 56.11 to 89.00%, respectively (Fig. 5E).

Several reservoir units of well A-7 display particularly favorable hydrocarbon saturation. Reservoir A10 has the highest Shc (94.31%) and a low Sw of only 5.69%, while A2 also exhibits high Shc (90.07%) and very low Sw (9.93%). reservoir units A1, A14, A13, and A12 likewise show Shc values exceeding 73% (Table 1). Conversely, A7 has high water saturation (87.79%) and low hydrocarbon saturation (12.21%), suggesting a water-dominated interval despite its relatively favorable porosity.

The reservoir units of well B-14 generally maintain relatively high hydrocarbon saturation, ranging from 56.11 to 89.00% (Table 1), despite their lower porosity and permeability. Reservoir unit B3 exhibits the highest Shc (89.00%), whereas unit B8 has the lowest value (56.11%). Overall, the saturation profiles indicate that hydrocarbon charge extends through both reservoir groups, although the quality and producibility of the deeper reservoir units of well B-14 are more strongly limited by their poorer petrophysical properties.

4.3 Gas distribution and hydrocarbon indications

Gas measurements show a marked contrast between the reservoir units of well A-7 and B-14 (Fig. 5F). Total gas concentrations in the reservoir units of well A-7 range from 2,846 to 17,778 ppm, averaging approximately 9,483 ppm. In contrast, the reservoir units of well B-14 contain only 430-1,368 ppm, averaging approximately 849 ppm (Table 2).

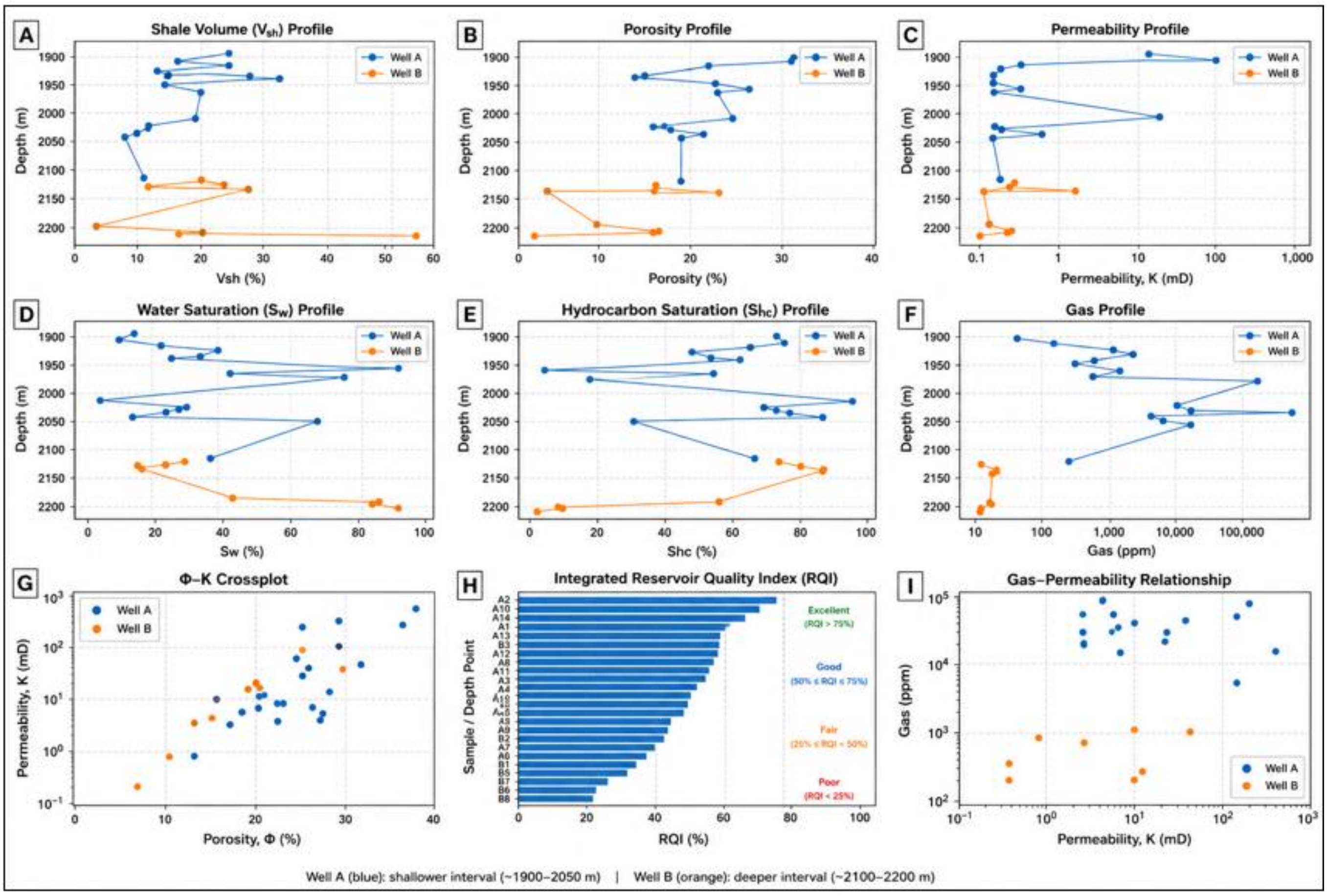

Figure 5: Integrated petrophysical evaluation and reservoir quality assessment of the Sokor-1 Formation: (A) shale volume (Vsh) profile; (B) porosity profile; (C) permeability profile; (D) water saturation (Sw) profile; (E) hydrocarbon saturation (Shc) profile; (F) gas concentration profile; (G) porosity-permeability (Φ-K) crossplot; (H) integrated Reservoir Quality Index (RQI); and (I) gas-permeability relationship.

The highest gas concentration occurs in reservoir units: A12 (17,778 ppm), followed by A9 (16,855 ppm), A11 (12,575 ppm), A15 (12,595 ppm), and A10 (11,887 ppm). In comparison, the reservoir units of well B-14 show substantially lower gas concentrations, with the maximum occurring at B3 (1,368 ppm). This pronounced contrast indicates a significantly stronger hydrocarbon/gas presence in the well A-7 reservoir system.

The gas-permeability crossplot (Fig. 5I) does not show a simple linear relationship between permeability and gas concentration. Several intervals with moderate or low permeability contain relatively high gas concentrations, whereas some high-permeability intervals do not correspond to the highest gas values. This suggests that gas occurrence is controlled by a combination of hydrocarbon charge, saturation, pore-fluid distribution, and reservoir architecture, rather than permeability alone.

Table 2: Gas data from reservoirs of the Sokor-1 Formation

Wells	Reservoir Units	Depth (m)		Gas (ppm)							
		From	To	C1	C2	C3	IC4	NC4	IC5	NC5	Total
Well A-7	A1	1890	2687	2687	81	50	28	0	0	0	2846
	A2	1898	4627	4627	181	86	42	28	0	0	4964
	A3	1906	7297	7297	498	272	68	49	37	23	8244
	A4	1911	7992	7992	658	427	93	66	41	17	9294
	A5	1921	6287	6287	326	257	88	69	49	25	7101
	A6	1924	5409	5409	296	155	59	49	17	15	6000
	A7	1933	7769	7769	326	174	80	63	44	24	8480
	A8	1943	6518	6518	200	115	79	69	31	19	7031
	A9	1948	16223	16223	313	147	62	63	27	20	16855
	A10	1987	9665	9665	1325	650	110	75	38	24	11887
	A11	1998	10319	10319	1379	631	91	105	27	23	12575

Paper ID: SR26823144710 DOI: https://dx.doi.org/10.21275/SR26823144710

	A12	2001	14769	14769	1792	909	113	137	31	27	17778
	A13	2005	8750	8750	1031	456	77	0	0	0	10314
	A14	2013	9607	9607	970	357	66	0	0	0	11000
	A15	2017	10927	10927	1164	428	76	0	0	0	12595
	A16	2092	4233	4233	253	149	81	46	0	0	4762
	Average values			8317	675	329	76	51	21	14	94,82,875
	B1	2098	2100	355	57	68	57	0	0	0	537
Well B-14	B2	2105	2109	970	86	100	68	68	31	0	1323
	B3	2110	2112	978	87	104	70	71	31	27	1368
	B4	2114	2116	776	74	91	63	63	31	20	1118
	B5	2181	2183	885	63	57	0	0	0	0	1005
	B6	2192	2194	524	0	0	0	0	0	0	524
	B7	2196	2197	483	0	0	0	0	0	0	483
	B8	2202	2204	430	0	0	0	0	0	0	430
	Average values			6,75,125	45,875	52,5	32,25	25,25	11,625	5,875	848,5

4.4 Integrated reservoir quality

The integrated Reservoir Quality Index (RQI) provides a combined assessment of the reservoir properties (Fig. 5H). The ranking indicates considerable heterogeneity among the analyzed intervals. The highest RQI values are associated predominantly with the reservoir units of well A-7, particularly A1, A2, A10, A13, and A14, whereas the lowest RQI values occur mainly in the deeper reservoir units of well B-14, especially B6-B8. The RQI distribution therefore confirms the individual petrophysical observations: the best reservoir quality is concentrated in the shallower reservoirs of well A-7, where relatively high porosity and permeability are accompanied by moderate shale content and favorable hydrocarbon saturation. Conversely, the deeper reservoir units of well B-14 generally exhibit reduced pore volume and flow capacity, resulting in lower integrated reservoir quality.

5. Discussion

5.1 Controls on reservoir quality

The results demonstrate that reservoir quality in the Sokor-1 Formation is strongly heterogeneous, as documented by Amadou et al. (2021b) and Ari et al. (2026), and varies systematically between the A and B reservoir groups. The superior quality of the reservoir units in well A-7 is principally associated with higher porosity, greater permeability, and generally lower shale content. Better sorting and larger grain size can enhance permeability by promoting more effective pore connectivity (Ma, 2019). The positive porosity-permeability relationship further indicates that preservation of interconnected pore space is an important control on fluid-flow capacity. This relationship also suggests that porosity and permeability are influenced by related geological controls, particularly the characteristics and connectivity of pore-throat systems (Nelson et al., 1994).

In contrast, the deterioration of reservoir properties in the deeper reservoir units of well B-14 is associated with increased argillaceous content, reduced pore volume, and poorer pore connectivity. The most unfavorable reservoir conditions occur in intervals characterized by high shale content and low porosity and permeability (Table 1). These characteristics are unfavorable for effective hydrocarbon production despite the presence of hydrocarbons.

Porosity generally decreases with increasing depth (Fig. 5B), suggesting that progressive burial compaction is an important control on porosity reduction, with lithofacies also exerting a significant influence (Genik, 1993; Ketzer et al., 2009). However, the observed variability indicates that depth alone does not determine reservoir quality. Some relatively deep intervals retain favorable petrophysical properties, whereas certain shallower intervals exhibit reduced permeability or higher water saturation. This variability highlights the importance of lithological heterogeneity and diagenetic modification in controlling the preservation, connectivity, and fluid-flow efficiency of pore systems.

5.2 Hydrocarbon saturation and reservoir effectiveness

The high hydrocarbon saturation (Shc) observed in many reservoir units indicates substantial hydrocarbon occupancy of the pore system. However, high hydrocarbon saturation does not necessarily imply equally high reservoir productivity. For example, the contrast between reservoir units A14 and B8 illustrates that hydrocarbon presence alone is insufficient to define reservoir effectiveness. A14 combines high hydrocarbon saturation with favorable porosity and permeability, whereas B8 retains appreciable hydrocarbon saturation but exhibits very low permeability (Table 2), indicating that hydrocarbons may be present but have limited flow capacity.

This distinction is important for reservoir evaluation because hydrocarbon saturation primarily reflects fluid occupancy, whereas porosity and permeability govern storage capacity and fluid deliverability (Ma, 2019). Therefore, the most prospective reservoir units are those in which high hydrocarbon saturation coincides with favorable porosity and permeability. This integrated interpretation provides a more reliable basis for distinguishing hydrocarbon-bearing intervals from intervals with effective production potential.

5.3 Relationship between gas occurrence and reservoir properties

The strong gas enrichment observed in the reservoirs of well A-7, particularly in reservoir units A9-A15, broadly coincides with favorable hydrocarbon saturation. However, the absence of a consistent gas-permeability relationship indicates that gas concentration cannot be interpreted solely as an indicator of reservoir quality.

The contrast between A9 and A2 illustrates this relationship: A9 exhibits substantial gas enrichment despite relatively low permeability, whereas A2 has the highest permeability but a comparatively lower gas concentration (Tables 1 and 2). This contrast indicates that gas concentration is more closely related to hydrocarbon charge and fluid accumulation than to permeability alone. Although permeability influences the capacity of hydrocarbons to flow through the reservoir, gas concentration also reflects the magnitude and distribution of hydrocarbons retained within the pore system. Consequently, gas concentration should be interpreted together with hydrocarbon saturation, porosity, and permeability when evaluating reservoir potential.

5.4 Implications of the integrated RQI

The Reservoir Quality Index (RQI) provides a more comprehensive assessment of reservoir quality than any individual petrophysical parameter because it integrates the effects of effective porosity and permeability. The predominance of high-RQI reservoir units in well A-7 indicates that these intervals constitute the principal reservoir targets within the studied section.

In contrast, the reservoirs of well B-14, particularly units B6-B8, exhibit lower reservoir potential because of their limited porosity and permeability. Nevertheless, their relatively high hydrocarbon saturation indicates that they should not be classified as non-reservoir solely on the basis of their fluid content. Rather, these intervals may represent hydrocarbon-bearing but low-productivity zones, potentially corresponding to tight or marginal reservoir intervals.

5.5 Integrated Reservoir Quality Interpretation

Overall, the integrated results reveal a vertically heterogeneous reservoir system, with reservoir quality generally decreasing from the units encountered in well A-7 toward those in well B-14. The most favorable reservoir conditions occur where relatively low shale content, high effective porosity, favorable permeability, low water saturation, and high hydrocarbon saturation coincide. This combination reflects the preservation of an effective pore system capable of providing both hydrocarbon storage and fluid-flow capacity.

The observed reservoir heterogeneity reflects the combined influence of depositional and post-depositional processes. Variations in facies and lithological composition exert primary controls on pore-space development, while burial compaction and diagenetic modification affect pore preservation and connectivity. Consequently, depth alone does not adequately explain the spatial variation in reservoir quality. Intervals with similar burial depths may exhibit markedly different petrophysical properties because of differences in lithology, shale content, grain characteristics, and diagenetic history.

Hydrocarbon distribution shows an additional degree of complexity. High hydrocarbon saturation and gas concentration indicate effective hydrocarbon charge and pore occupancy, but they do not necessarily correspond to high reservoir productivity. Productive potential depends on the combined effects of hydrocarbon saturation, effective porosity, and permeability, with permeability being particularly important for fluid deliverability. Therefore, hydrocarbon-bearing intervals with poor pore connectivity should be distinguished from intervals that combine hydrocarbon charge with favorable flow properties.

The integrated interpretation of petrophysical properties, saturation parameters, gas measurements, and Reservoir Quality Index (RQI) provides a more robust basis for evaluating reservoir potential than any individual parameter considered independently. This approach highlights the importance of identifying intervals where favorable pore-system characteristics coincide with effective hydrocarbon occupancy and, consequently, provides a more reliable basis for ranking prospective reservoir zones within the Sokor-1 Formation.

6. Conclusion

The integrated petrophysical and gas-log evaluation indicates that the Sokor-1 Formation in the Agadi Prospect contains heterogeneous but locally favorable hydrocarbon reservoirs. Reservoir intervals in well A-7 generally show better porosity, permeability, gas indications, and overall reservoir quality than the deeper intervals investigated in well B-14. Reservoir performance is principally associated with pore-space preservation and connectivity, with additional influence from shale content, lithological heterogeneity, and diagenetic modification. Units A1, A2, A10, A13, and A14 represent the most favorable intervals based on their combined reservoir properties and hydrocarbon saturation. In contrast, several deeper B-14 intervals contain hydrocarbons but have comparatively limited flow capacity. Integration of petrophysical properties, fluid saturation, gas measurements, and reservoir-quality assessment therefore provides a useful basis for reservoir zonation and identification of prospective intervals within the Sokor-1 Formation.

Funding
Funding for this research was provided by the African Union Commission through the Pan African University Life and Earth Sciences Institute (including Health and Agriculture), Ibadan, Oyo State, Nigeria.

Declaration of competing interests
The authors declare that they have no known conflicts of interest that could influence this paper.

Acknowledgments
We express our sincere gratitude to the African Union, which supported this research through a Ph. D. scholarship and a research grant awarded to the first author. The authors would also like to express their gratitude to the Nigerien Ministry of Petroleum, Niamey, for providing the data and for granting permission to publish this paper. The authors would like to express their sincere thanks to all the anonymous reviewers for their immense contribution to the improvement of this paper.

References

[1] Amadou, H., Ehirim, C. N., & Dagogo, T. (2021a). Rock physics diagnostic of Eocene Sokor-1 reservoir in Termit subbasin, Niger. In *Journal of Petroleum Exploration and Production Technology* (Vol. 11, Number 9, pp. 3361-3371). Springer Science and Business Media Deutschland GmbH. https://doi.org/10.1007/s13202-021-01259-2

[2] Amadou, H., Ehirim, C. N., & Dagogo, T. (2021b). Well-Based Quantitative Reservoir Characterization of Eocene Sokor-1 Formation, Termit Basin, Niger. *International Journal of Geosciences*, *12*(02), 159-169. https://doi.org/10.4236/ijg.2021.122010

[3] Amaefule, J. O., Altunbay, M., Tiab, D., Kersey, D. G., & Keelan, D. K. (1993). Enhanced reservoir description: using core and log data to identify hydraulic (flow) units and predict permeability in uncored intervals/ wells. *Proceedings - SPE Annual Technical Conference and Exhibition*, *Omega*, 205-220. https://doi.org/10.2118/26436-ms

[4] Archie, G. E. (1942). The Electrical Resistivity Log as an Aid in Determining Some Reservoir Characteristics. *SPE Reprint Series*, (55), 9-16. https://doi.org/10.2118/942054-g

[5] Ari, M. A. I., Nton, M. E., Harouna, M., & Moussa, H. A. (2024). Reservoir fluid characterization of the Sokor1 Formation, Fana tectonic unit, Termit Basin, southeastern Niger Republic. *Arabian Journal of Geosciences*, *17*(5), 1-18 https://doi.org/10.1007/s12517-024-11918-3

[6] Ari, M. A. I., Nton, M. E., & Harouna, M. (2026). Petrophysical Evaluation of Reservoir Quality from Well Logs of the Sokor-1 Formation , Termit Basin , Southeastern Niger. *International Journal of Innovation and Applied Studies*, *48*(3), 1041–1052

[7] Amaefule, J. O., Altunbay, M., Tiab, D., Kersey, D. G., & Keelan, D. K. (1993, October). Enhanced reservoir description: using core and log data to identify hydraulic (flow) units and predict permeability in uncored intervals/wells. In *SPE Annual Technical Conference and Exhibition?* (pp. SPE-26436). SPE

[8] Bosworth, W. (1992). Mesozoic and early Tertiary rift tectonics in East Africa. *Tectonophysics*, *209*(1-4), 115-137. https://doi.org/10.1016/0040-1951(92)90014-W

[9] Cannon, S. (2015). Petrophysics: a practical guide. John Wiley & Sons

[10] Chang, E., & Zung, L. S. (2017). 3D Reservoir Characterization of Field Deta, Termit Basin, Niger. *Icipeg 2016*, 323-335. https://doi.org/10.1007/978-981-10-3650-7

[11] Darling, T. (2005). Well Logging and Formation Evaluation. In *Well Logging and Formation Evaluation*. https://doi.org/10.1016/B978-0-7506-7883-4.X5000-1

[12] Genik, G. J. (1993). Petroleum Geology of Cretaceous-Tertiary Rift Basins in Niger, Chad, and Central African Republic. *The American Association of Petroleum Geologists*, *77210-4778*, 30

[13] Hamma, A. M, Harouna, M. (2019). Diagenesis and reservoir quality evolution of the paleogene sokor1 sandstones in the agadem block, termit basin, eastern Niger. *Int J Adv Geosci*, *7*(2), 147

[14] Hamma, A. M., Dodo Bohari, A., Ibrahim Maharou, H., Ibrahim Ari Maina, A., & Harouna, M. (2022). Effect of Oil in Place on Sandstone Reservoir Quality of Dibeilla Prospect, Termit Basin, Niger: Insight from Pre-Stack Seismic Inversion and Diagenesis. *International Journal of Science and Research (IJSR)*, *11*(12), 1203-1226. https://doi.org/10.21275/sr221227121605

[15] Harouna, M., & Philp, R. P. (2012). Potential petroleum source rocks in the Termit Basin, Niger. *Journal of Petroleum Geology*, *35*(2), 165-185. https://doi.org/10.1111/j.1747-5457.2012.00524.x

[16] Ji-Lin, F. U., Zhi-Hua, S. U. N., & Kang-Ning, L. I. U. (2012). The study on sequence stratigraphy and sedimentary systems of Paleogene in Agadem Block. Earth Science Frontiers (China Universsity Og Geoscience (Beijing): Pekin University, 19(1), 10

[17] Ketzer, J. M., Morad, S., & Amorosi, A. (2009). Predictive Diagenetic Clay-Mineral Distribution in Siliciclastic Rocks within a Sequence Stratigraphic Framework. In *Clay Mineral Cements in Sandstones* (Number March). https://doi.org/10.1002/9781444304336.ch2

[18] Krygowski, D. (2004). Basic well log analysis. American Association of Petroleum Geologists

[19] Larionov, M. (1969). Application of factor analysis to well logging data. *Earth Science Journal*, *1*(1), 113-123

[20] Ma, Y. Z., & Zhang, X. (2019). Quantitative geosciences: Data analytics, geostatistics, reservoir characterization and modeling (p. 640). Cham: Springer International Publishing

[21] Nasaruddin, M. N., Zung, L. S., & Md Rafek, A. G. (2017). Petrophysical Analysis of E5 sand group of Sokor Formation, Termit Basin, Niger. *IOP Conference Series: Earth and Environmental Science*, *88*(1), 9. https://doi.org/10.1088/1755-1315/88/1/012003

[22] Nelson, C. S., Kamp, P. J. J., & Young, H. R. (1994). Sedimentology and petrography of mass-emplaced limestone (Orahiri Limestone) on a late Oligocene shelf, western North Island, and tectonic implications for eastern margin development of Taranaki Basin. *New Zealand Journal of Geology and Geophysics*, *37*(3), 269-285. https://doi.org/10.1080/00288306.1994.9514621

[23] Philip, J. (1993). Paléoenvironnements cénomaniens tardifs (94–92 Ma). Atlas Tethys palaeoenvironmental maps, Explic

[24] Schlumberger, L. I. (1989). Principles and Application: Schlumberger Wireline and Testing. *Houston, Texas*, 21-89

[25] Schull, T. J. (1988). Rift basins of interior Sudan: petroleum exploration and discovery. *American Association of Petroleum Geologists Bulletin*, *72*(10), 1128-1142. https://doi.org/10.1306/703c9965-1707-11d7-8645000102c1865d

[26] Tixier, M. (1949). Evaluation of permeability from electric-log resistivity gradients. *The Oil and Gas Journal*, *16*, 113-133

[27] Wan, L., Liu, J., Mao, F., Lv, M., & Liu, B. (2014). The petroleum geochemistry of the Termit Basin, Eastern Niger. *Marine and Petroleum Geology*, *51*, 167-183. https://doi.org/10.1016/J.MARPETGEO.2013.11.006

[28] Wang, X., Wan, L., Jiang, Z., Liu, R., Wang, X., Tang, W., ... & Xu, W. (2017). Controlling factors and

accumulation model of hydrocarbon reservoirs in the Upper Cretaceous Yogou formation, Koulele area, Termit basin, Niger. Journal of Earth Science, 28(6), 1126-1134

[29] Wilson, M., & Guiraud, R. (1992). Magmatism and rifting in Western and Central Africa, from Late Jurassic to Recent times. *Tectonophysics*, *213*(1-2), 203-225. https://doi.org/10.1016/0040-1951(92)90259-9

[30] Zanguina, M., Bruneton, A., & Gonnard, R. (1998). An introduction to the petroleum potential of Niger. *Journal of Petroleum Geology*, *21*(1), 83-103. https://doi.org/10.1111/j.1747-5457.1998.tb00647.x

[31] Zhao, N., Huang, J., Ning Zhao & Jiangqin Huang, Zhao, N., & Huang, J. (2019). Sedimentary

[32] Characteristics and Lithological Trap Identification of Distant Braided Delta Deposits: A Case on Upper Cretaceous Yogou Formation of Sedimentary Characteristics and Lithological Trap Identification of Distant Braided Delta Deposits: A Case. *ASEG Extended Abstracts ISSN:*, *0586*, 9. https://doi.org/10.1071/ASEG2018abT7